Korean J. Chem. Eng., 33(10), 2998-3010 (2016)
DOI: 10.1007/s11814-016-0165-8

pISSN: 0256-1115
eISSN: 1975-7220

Process modeling and optimization studies of high pressure membrane separation of CO_2 from natural gas

Jimoh Kayode Adewole*, and Abdul Latif Ahmad*,†**

*School of Chemical Engineering, Engineering Campus, Universiti Sains Malaysia,
14300 Nibong Tebal, Seberang Prai Selatan, Pulau Pinang, Malaysia
**Center for Integrative Petroleum Research, King Fahd University of Petroleum & Minerals,
Dhahran 31261, Saudi Arabia
(*Received 23 December 2015 • accepted 15 June 2016*)

Abstract−Process design and optimization methodology for high pressure membrane removal of CO_2 from natural gas was developed. An approximate model based on plasticization pressure and permeability parameters at plasticization was proposed for quick evaluation of membrane materials for the high pressure operation. The model was derived by applying the partial immobilization assumption to the fundamental model of solution - diffusion mechanism along with a modified upper-bound curve. About ninety membranes obtained from literature were used to illustrate this methodology. The best three were selected for detailed process modeling and optimization. Process optimization was achieved via non-linear programming constraint optimization model. Gas processing cost was used as the objective function, while plasticization pressure and the CO_2 concentration in the feed were used as the constraints. Membrane of 6FDA-durene had the lowest annual gas processing cost while 6FDA-DAM : DABA 2 : 1 had the highest optimum product purity.

Keywords: Penetrant-induced Plasticization, Plasticizing Feed Stream, Productivity Loss, Permeability Parameter, Non-linear Programming

INTRODUCTION

The boost in technological innovation in the 1960s and 1970s led to large-scale application of membranes in gas separation [1]. In 1989, membrane materials for acid gas separation ranked as the twelfth out of the 38 research topics constituting the research needs in the membrane separation industry by a group of six membrane experts [2]. Consequently, use of membrane in CO_2 removal from natural gas has grown about tenfold since 1990 to become a $150 million/year business. However, amine absorption still has 90% of the natural gas (NG) processing market because today's membranes are not good enough to displace the use of absorption [2-4]. High pressure operations have been suggested as one of the means to improve the competitiveness of membrane for CO_2 removal [5,6]. Unfortunately, the penetrant induced plasticization behavior of certain condensable components of natural gas, such as CO_2, still remains a difficult challenge that is limiting membrane separation from achieving its full potential in natural gas processing, especially at high pressure.

By definition, plasticization is a pressure-dependent phenomenon caused by the dissolution of certain penetrants within the polymer matrix, which disrupts the chain packing and enhances intersegmental mobility of polymer chains [7,8]. Penetrant-induced plasticization of gas separation membranes by CO_2 has been reported to permanently alter their performance and consequently increase the materials' susceptibility to failure [9,10]. Usually, the permeability of glassy polymer decreases with increase in feed gas pressure. For plasticizing penetrants, continuous increase in the feed gas pressure beyond a certain critical value causes a gradual increase in permeability. The pressure at which the permeability starts to increase with increasing pressure is referred to as the plasticization pressure. Therefore, to minimize the effect of plasticization, high pressure membrane operation needs to be well managed.

A number of studies on optimization of membrane based gas separation processes have been published. A detailed economic study of membrane gas separation was published by Spillman [11]. According to the author, early comparison of membrane processes with other separation methods has focused on non-optimized single stage operations. This often leads to incorrect conclusions on the performance of single stage membrane configuration.

Process optimization studies primarily focusing on membrane separation of CO_2 from natural gas have also been published. For example, Bhide and Stern did a study on the process configurations and optimization of operating conditions of membrane based acid gases removal from natural gas [12]. Qi and Henson did modeling and optimization of spiral-wound membrane system for CO_2/CH_4 separation [13,14]. Hao et al. performed process design and economic studies of CO_2 selective membranes [15,16]. One of their conclusions was that a single stage membrane is the most economical process configuration for upgrading natural gas with CO_2 concentration up to 40 mol%, and small amount of H_2S up to 8 mol%. Moreover, previous optimization studies were extended by Datta

†To whom correspondence should be addressed.
E-mail: chlatif@usm.my

and Sen [17] using a rigorous process model and the Broyden-Fletcher-Goldfarb-Shanno (BFGS) optimization algorithm. Several configurations, including those that were reported in previous literatures, were compared. The best of these configurations were then optimized to find the best design variables. The results obtained by the authors showed that a two-stage optimum configuration had almost the same economy as that of three-stage configuration. Parametric evaluation of membrane based separation process for removal of CO_2 from NG was performed by Yang et al. [18]. It was concluded that using membrane with selectivity higher than 50, a CH_4 recovery higher than 98% and product purity greater than 98% can be achieved by the single stage system.

However, the same separation can be achieved by using a membrane with selectivity of 20 by using two-stage membrane system. Safari et al. [19] developed a model that incorporates the feed pressure and temperature. The model was used to simulate NG sweetening, and the effects of feed temperature, feed pressure and permeate pressure on membrane performance were examined. It was concluded that hydrocarbon losses below 2% can be achieved by using a two-stage membrane process. Ahmad et al. used process simulation, design and optimization of membrane separation system for CO_2 removal from natural gas [20], using the cross flow model that was executed in Aspen HYSYS user defined unit operation. Technical and economic analysis of CO_2 removal from natural gas using amine absorption and membrane was conducted by Peters et al. [21] based on gas processing cost and total capital investment. Both single and two-stage systems were investigated and the conclusion was that single stage was not suitable for feed stream containing low CO_2 content due to low CO_2 recovery. Table 1 shows details of the results of comparison between amine absorption and membrane separation technologies for CO_2 separation from feed stream of 2.90% CO_2 and 97.10% CH_4.

In all the mentioned membrane based optimization studies, models with constant gas transport permeability coefficients were employed. Such models are based on assumptions which cannot be justifiably applied over a wide range of operating conditions [22]. Therefore, the present paper proposes a new optimization methodology that takes into account the variation of gas permeability with pressure and the plasticization pressure of the membrane. A model based procedure was applied to select suitable polymeric membrane materials by considering the productivity loss, plasticization pressure and the permeability parameters at plasticization. These criteria were used in conjunction with the Robeson upper bound curve that was modified for high pressure gas separation process.

The most common and the simplest membrane design is the single stage arrangement without recycle [21]. Also, a single stage configuration without recycle has been reported to be the optimum process configuration in gas separation study such as oxygen enrichment [23]. Single stage provides the lowest capital cost; however, it can result in higher than necessary product losses [11]. Consequently, industrial requirements for improved product purity and product recovery are usually met by using recycle streams or multistage configurations. However, the addition of extra stages often leads to increase in both the capital and the operating costs.

Table 1. Comparison of gas processing cost of amine absorption and membrane technology

	Amine absorption	Membrane (1-satge)	Membrane (2-stage)
GPC ($/mscf product)	0.18	0.08	0.12

In the present work, it was determined that huge saving is possible by installing a plasticization resistant membrane in an area which involves high pressure operations or points within the gas processing plant where compressors already exist. Moreover, natural gas is often obtained directly from gas wells at pressure ranging from 20 to 83 bar and compositions between 4 and 50% CO_2 [19,24,25]. Thus, membrane based gas separation can be enhanced by a combination of optimized single stage configuration and selection of suitable membrane materials. The higher product losses that are often associated with single stage configuration can be minimized by increasing the feed pressure and using materials of excellent plasticization resistance coupled with gas transport properties. It should be emphasized that our primary objective was to outline a methodology for the optimization of high-pressure gas separation processing where gas permeability changes with increase in feed pressure.

ANALYSIS OF MEMBRANE MATERIALS' PERFORMANCE FOR HIGH PRESSURE OPERATIONS

An approximate model that is based on the dual-sorption and total immobilization model was proposed to formulate the permeability-pressure relationship. This relationship was subsequently used for selecting the most suitable membrane material. The main property of membranes used in separation applications is the ability to control permeation of different species through them. Solution-diffusion was first used to explain permeation of gases through polymeric membranes in the 1940s, and this has remained the most commonly used model for describing gas transport in non-porous dense membrane materials [26]. The mechanism of gas permeation in polymers can be explained in three successive stages [27,28]:

i. Dissolution/sorption of gas at the high pressure side of the membrane materials

ii. Gas diffusion through the membrane on concentration gradients

iii. Gas desorption at the low pressure side of the membrane

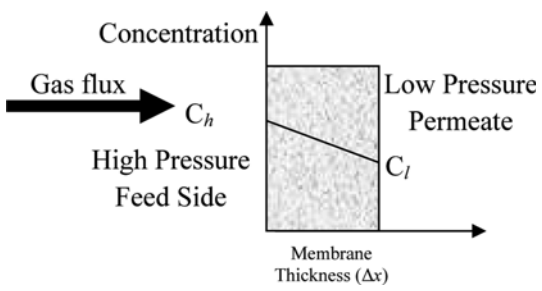

Fig. 1. Schematic of gas transport in non-porous membrane.

materials

Fig. 1 is a representative diagram depicting the flow of gas into a polymeric membrane. Gas flux into such membrane can be defined as the quantity of diffusing gas (Q) which crosses the membrane of area (A), during a specified time (t).

Mathematically:

$$J=\frac{Q}{At} \tag{1}$$

By analogy with heat transfer by conduction, Eq. (1) can be represented by Fick's first law. The steady state unidirectional case of this law is:

$$J_x=-D\frac{\partial C}{\partial x} \tag{2}$$

The simplification in the above equation is valid in the present situation since the thickness of the membrane is always much smaller than the diameter. For most gases, D is often assumed to be constant. However, for highly sorbing gases such as CO_2 and high hydrocarbon, diffusion is concentration dependent. Thus, the flux can be written as:

$$J_x=-D(C)\frac{\partial C}{\partial x}, \tag{3}$$

where C is the concentration of the diffusing species across the membrane. This is indeed the fraction of the diffusing species with certain level of mobility.

Many studies are available on the historical perspective and theory of gas transport through polymeric membranes. However, the two most commonly applied theories for analyzing gas permeation in polymeric membranes are the free volume theory and the dual sorption model. The dual sorption model postulates that the total concentration, C, of gas dissolved in a glassy polymer at equilibrium pressure, p, is the sum of two thermodynamically distinct contributions, which can be represented thus [29]:

$$C=C_D+C_H, \tag{4}$$

where C_D is the penetrant concentration due to ordinary dissolution (which obeys Henry's law) and C_H is the concentration due to micro cavities or holes (which obeys the Langmuir Isotherm).

Henry's law is mathematically expressed as:

$$C_D=k_Dp, \tag{5}$$

with k_D as the solubility coefficient in the Henry's law limit (which is the reciprocal of Henry's law constant). Similarly, the Langmuir is represented as:

$$C_H=\frac{C'_Hbp}{1+bp} \tag{6}$$

C'_H is the saturation concentration of the penetrant species in the polymer micro cavities, b is the hole affinity constant. Thus, the total concentration can be obtained by substituting (5) and (6) into (4). That is:

$$C=k_Dp+\frac{C'_Hbp}{1+bp} \tag{7}$$

One of the three stages involved in the mechanism of gas transport through polymeric membranes is the diffusion of penetrant gas through the membrane as highlighted earlier. The mobile (diffusing) fraction of the total concentration can be described using one of the following models:

i) Total immobilization model

ii) Partial immobilization model

The total immobilization assumed that only the concentration associated with the Henry's has some finite mobility. Gas species in the Langmuir sorption are totally immobilized.

$$C_{mob}=C_D \tag{8}$$

For the partial immobilization model, the concentration of the diffusing gas species was assumed to be the sum of the penetrant associated with C_D and a fraction F of the gas species associated with C_H. That is:

$$C_{mob}=C_D+FC_H, \tag{9}$$

where

$$F=\frac{D_H}{D_D} \tag{10}$$

Thus, the fraction (1−F) of the Langmuir is totally immobilized [30,31].

To select the most suitable model for the polymers under consideration in this work, experimental values of F for various kinds of polymers were examined. Reported literature data of F for some polymers are shown in Table 2. A look at this table reveals that the sorption behaviour of some glassy polymers such as the one under consideration in this work can be approximated using total immobilization model. Combining the total immobilization assumption

Table 2. Dual sorption model data for various kinds of polysulfone (PSF), polyethersulfones (PES), phenylene oxide (PPO), polycarbonate and polyimides [33-40]

Polymer	$D_D\times10^8$ (cm^2/s)	$D_H\times10^8$ (cm^2/s)	F
6FDA-1,5-NDA	10.1	0.665	0.065
TM-PSF	22	1.54	0.070
DM-PSF	2.8	0.179	0.064
DM-PSF-Z	1.62	0.077	0.048
TMHF-PSF	35.5	2.97	0.084
PSF	4.64	0.575	0.124
Udel PSF	4.4	0.46	0.105
HF-PSF	8.9	1.07	0.120
PSF-F	4.46	0.763	0.171
PES	2.27	0.34	0.150
PES (Nitrated)	2.16	0.4	0.185
PPO	36.8	3.68	0.100
PPO (36% Brominated)	36.9	2.69	0.073
PPO (91% Brominated)	48.2	3.3	0.068
Polycarbonate	6.22	0.485	0.078
Poly ether ether ketone	1.07	0.19	0.181
Polyetherimide	1.14	0.07	0.063

with the steady state form of the Fick's law, the steady state flux can be denoted as:

$$J_x \approx -D(C_{mob})\frac{\partial C_{mob}}{\partial x} \tag{11}$$

One of the most widely used expressions for the concentration dependency of diffusion coefficient through polymer is [32]:

$$D(C_{mob})=D_o \exp(\varphi C_{mob}) \tag{12}$$

The gas permeation coefficient across a non-porous membrane of thickness l is often defined as:

$$P=\frac{J_s l}{p_h} \tag{13}$$

This is for a permeation experiment which is performed in such a way that $p_h >> p_l$. This condition fit very well with the high pressure operations.

Using the following boundary conditions, penetrant permeability through a glassy polymeric membrane is obtained as shown below.

x=0, $C_{mob}=C_{mobh}$ (at the high pressure feed side where, $p=p_h$)

x=l, $C_{mob}=C_{mobl}\approx 0$, (at the low pressure permeate side where, $p=p_l=0$)

$$P=\frac{D_o(\exp(\varphi C_{mobh})-1)}{\varphi \quad p_h} \tag{14}$$

The permeability defined by Eq. (14) is for concentration dependent diffusion [41]. Expanding Eq. (14) using Taylor expansion, the relation between the plasticization pressure and permeability at plasticization as represented by Eq. (15) is obtained:

$$P(p)=a_1p^2+a_2p+a_3 \tag{15}$$

where

$$a_1=\frac{D_o\varphi^2 k_D^3}{6} \tag{16}$$

$$a_2=\frac{D_o\varphi k_D^2}{2} \tag{17}$$

$$a_3=D_o k_D \tag{18}$$

The coefficients are used to formulate some criteria that were used in conjunction with the Robeson upper bound curve for membrane material selection.

1. Plasticization Pressure and Permeability Parameters at Plasticization Pressure

Plasticization pressure is the pressure at which gas permeability exhibits a minimum value [7,9]. Thus, plasticization pressure can be obtained from the first derivative of Eq. (15). Thus

$$p_{pl}=\frac{-a_2}{2a_1} \tag{19}$$

Also, permeability at plasticization pressure is defined as:

$$P(p_{pl})=a_3-\frac{a_2^2}{4a_1} \tag{20}$$

where p_{pl} is the plasticization pressure (bar)

For most polymers, permeabilities of CH_4 are not always pressure dependent; thus a constant value can be taken [42]. On the other hand, some results have been reported where CH_4 permeabilities exhibit pressure dependent [10,19]. In such cases, permeability of CH_4 at plasticization is estimated by using Eq. (20). For binary gas mixture such as CO_2/CH_4, ideal separation factor at plasticization is given by:

$$\alpha_{CO_2\text{-}CH_4}=\frac{P_{CO_2}(p_{pl})}{P_{CH_4}(p_{pl})} \tag{21}$$

A plot of the plasticization pressure and permeability at plasticization of some polymers is shown in Fig. 2. Details of these polymers are presented elsewhere [10,24,33-37,43-54].

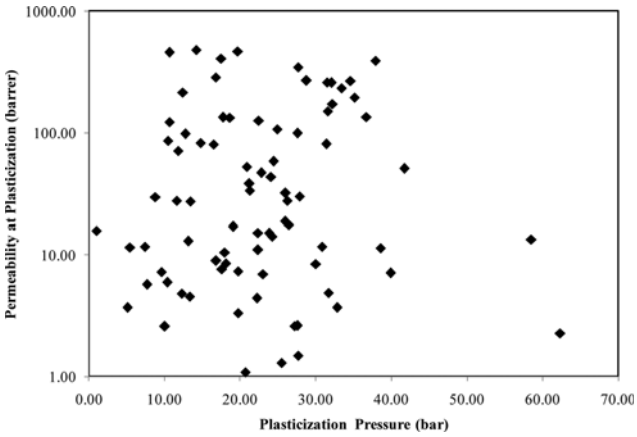

Fig. 2. Membrane performance based on plasticization pressure and permeability parameters at plasticization.

2. Productivity Loss at Plasticization Pressure

As explained earlier, the productivity (permeability) of polymeric membrane decreases with increase in pressure until the plasticization pressure is reached. The amount of decrease in the productivity is thus a very important economic parameter that needs to be evaluated to improve membrane competitiveness with other separation processes. An expression is developed to evaluate this loss as follows:

Permeability at zero pressure: $P(p_o)=a_3$ (22)

And permeability at plasticization pressure: $P(p_{pl})=a_3-\frac{a_2^2}{4a_1}$ (23)

Change in productivity at the plasticization pressure can be calculated as the difference between the initial and the final permeability (at plasticization pressure):

$$\Delta P=-\frac{a_2^2}{4a_1} \tag{24}$$

Percentage decrease in the productivity can be calculated by combining Eqs. (22) and (24). Thus:

$$\%\Delta P=-\frac{a_2^2}{4a_1a_3} \tag{25}$$

In this paper, Eq. (25) is referred to as productivity loss. For the development of novel polymeric membrane with high gas permeability for high pressure or processing of plasticizing feed stream,

there is the need to control the plasticization pressure and the productivity loss. Based on this, plasticization pressure and the accompanied productivity loss are evaluated. Table 3 illustrates plasticization pressure with respect to percentage absolute change in productivity. The table contains results obtained for more than eighty (80) polymeric membranes [10,24,33-36,43-53,55-66]. Data contained in this table were among those that were used to make a complete judgment in selecting membrane materials for high pressure CO_2

Table 3. Membrane plasticization pressure and productivity loss

Polymeric membrane samples	Estimated plasticization pressure (atm)	Productivity loss (%)
6FDA-1,5-NDA	25.99	33.26
6FDA-durene polyimide (Dense films)	10.64	41.99
Pure 2,6 dimethyl-1,4-poly (phenylene oxide)	19.06	63.88
Brominated 2,6 dimethyl-1,4-poly (phenylene oxide) 36%	23.87	69.43
Brominated 2,6 dimethyl-1,4-poly (phenylene oxide) 91%	24.09	54.72
Poly (ether ketone) 6H6F	19.71	29.05
Poly (ether ketone) 6F6H	23.04	32.58
Poly (ether ketone) 12F	17.98	32.33
6F-PAI-1	26.27	19.84
6F-PAI-2	30.81	24.61
6FPA-3	24.25	25.61
6FDA-DAM : DABA 2 : 1 (130 °C free acid)	10.69	20.58
6FDA-DAM : DABA 2 : 1 (220 °C free acid)	27.61	35.37
6FDA-DAM : DABA 2 : 1 (295 °C free acid)	31.41	34.17
6FDA-DAM : DABA 2 : 1 (100 °C CHDM)	8.79	10.82
6FDA-DAM : DABA 2 : 1 (220 °C CHDM)	26.46	36.25
6FDA-DAM : DABA 2 : 1 (295 °C CHDM)	41.69	41.06
6FDA-6FpDA/DABA 2 : 1 (Un-x-linked)	11.59	23.01
6FDA-6FpDA/DABA 2 : 1 (Un-x-linked)	11.59	23.01
6FDA-6FpDA/DABA 2 : 1 (Ethylene glycol cross - linked)	26.01	27.51
6FDA-6FpDA/DABA 2 : 1 (Aluminium cross -linked)	13.43	10.28
6FDA-ODA-TeMP-5.5%	38.56	67.73
6FDA-ODA-0	22.38	30.06
6FDA-ODA-5H	39.92	57.45
6FDA-ODA-TeMPD-O	20.92	16.66
TCDA-DADE	10.06	16.16
SPI-9	5.47	3.56
6FDA-DAMA : DABA (3 : 2) (180 °C)	12.76	15.46
6FDA-DAMA : DABA (3 : 2) (230 °C)	10.45	8.96
6FDA-D	19.69	28.92
6FDA-D4A1	16.80	30.71
6FDA-D4A1-400	36.70	45.80
6FDA-NDA	21.28	24.62
6FDA-NDA/azide (90-10)	22.36	27.00
6FDA-TMPDA	12.43	29.40
6FDA-TMPDA/azide (70-30)	21.22	29.96
6FDA-ODA	7.41	19.17
6FDA-DAM : DABA (2 : 1) (220 °C for 23 h)	35.10	39.43
6FDA-DAM : DABA (2 : 1) (220 °C for 23 h conditioned in 95 °C water	32.22	37.60
Tetramethylhexafluoro Polysulfone (TMHFPSF)	11.79	17.67
6FDA-DAMA : DABA (3 : 2) 370 1 h	37.91	22.39
6FDA-DAMA : DABA (3 : 2) 350 1 h	31.46	30.79
6FDA-DAMA : DABA (3 : 2) 330 1 h	32.09	23.41
6FDA-DAMA : DABA (3 : 2) 330 10 h	33.43	33.71
6FDA-DAMA : DABA (3 : 2) 330 20 h	34.60	36.70
6FDA-DAMA : DABA (3 : 2) 300 20 h	31.59	31.88

Table 3. Continued

Polymeric membrane samples	Estimated plasticization pressure (atm)	Productivity loss (%)
6FDA-DAMA : DABA (3 : 2) 220 24 h	22.47	21.15
6FDA-DAMA : DABA (3 : 2) 180 24 h	24.90	32.51
6FDA-DAMA : DABA (3 : 2) 120 24 h	17.71	27.07
SPEEK (Na) 1	13.36	4.14
SPEEK (Na) 2	30.00	17.61
SPEEK (Na) 3	58.50	7.16
Matrimid	17.59	15.72
Matrimid (7 Days X-Linked)	22.24	27.71
Matrimid (32 Days X-Linked)	27.20	29.94
Polycarbonate	18.11	31.57
poly(methyl methacrylate) PMMA	5.09	6.65
Cyclic Olefin Co polymer	7.72	9.65
6FDA-TeMPD DCM	28.76	63.58
6FDA-TeMPD THF	27.67	41.42
PDMC cross-linked at 220 °C	22.79	22.48
PDMC uncross-linked	1.01	0.07
Radel A PES (SPESII-H)	27.67	31.71
6FDA-2,6-DAT	27.88	32.87
6FDA-durene	14.17	13.43
Cross-linked 6FDA-durene	17.50	15.81
Polysulfone (Udel P3500)	32.83	26.07
Polyethersulfone (Ultrason E 6010P)	27.58	27.50
Polyetherimide (ULTEM 1000)	24.38	21.14
Bisphenol A Polycarbonate (Macrolon 3200)	31.71	35.03
Bisphenol Z Polycarbonate	20.71	21.70
Tetramethyl Bisphenol A Polycarbonate	13.13	15.74
Poly(2,6 dimethyl-p-phenylene) oxide	14.79	17.40
Polyimide (Matrimid 5218)	12.28	16.08
Copolyimide (P84)	27.50	7.80
Cellulose Acetate	10.41	10.63
Cellulose Triacetate	9.64	19.44
Polyimide (Matrimid 5218)	16.83	18.36
Polyhydroxyether	19.33	28.53
Polyhydroxyether+40 wt%Polyethersulfone	15.94	23.99
Polyhydroxyether+60 wt%Polyethersulfone	19.71	27.98
Torlon	33.75	9.38
Cross - linked 6FDA-DAMA_DAB 3 : 2	24.43	

removal from natural gas.

3. Modified Upper Bound Relationship for Plasticization Resistant Membrane Materials

An important discovery regarding a trade-off between permeability and selectivity was recognized by Robeson [67]. This relationship was mathematically represented as:

$$P_A = k\alpha_{AB}^{n} \quad (26)$$

where P_A is the permeability of the fast gas A, α_{AB} is the selectivity of the fast gas A with respect to the slow gas B. Also, k and n are constant parameters.

Following the pioneering work of Robeson [67] on the correlation of separation factor versus permeability for polymeric gas separation membranes, many authors (including Robeson) have published other reports on the upper bound relationship for evaluating membrane performance. Theoretical basis of the permeability-selectivity trade-off was presented by Freeman [68]. The empirical as well the theoretical aspects of the upper bounds was further revisited by Dal-Cin et al. [49]. Upper bound relationship was presented for proton exchange membranes by Robeson et al. [69]. To accommodate the permeability data of newly developed polymeric membrane materials, the upper bound curve for gas separation membranes was again revisited by Robeson [70]. Authors also developed an empirical correlation of gas permeability and permselectivity in polymers [48]. The effect of gas and polymer properties, such as free volume [71] and temperature, have also

been investigated [72]. Robeson recently published a study on the contributions of diffusion and solubility selectivities to the upper bound analysis for glassy gas separation membranes [73]. All these have been done for polymers usually used for low pressure membrane based gas separation. On the other hand, many polymers have been produced and tested for high pressure applications; however, there is no established model to measure their performance relative to other previously developed membranes. In this work, the Robeson upper-bound relationship was modified for the high pressure situation by incorporating the plasticization pressure. Thus:

$$P_A(p_l)=k(\alpha_{A/B}(p_{pl}))^n \quad (27)$$

where k is the front factor, the upper bound slope, $P_A(p_{pl})$ permeability of more permeable gas at plasticization pressure and $\alpha_{A/B}(p_{pl})$ is the ideal separation factor at plasticization pressure defined by Eq. (21).

Fig. 3 is a log-log plot of the ideal selectivity at plasticization pressure versus CO_2 permeability at plasticization pressure. Like the low pressure case, the figure displays an upper bound curve. There is a linear upper bound above which no polymeric membrane samples exist. Membranes close to the upper bound are mainly the 6FDA-polymers [24,74]. It is good that membranes for high pressure operation exhibit a balance between high plasticization pressures, high permeability parameters at plasticization, and very low productivity loss. Table 4 contains membrane materials that were selected for optimization studies based on the results from Figs. 2-3 and Table 3.

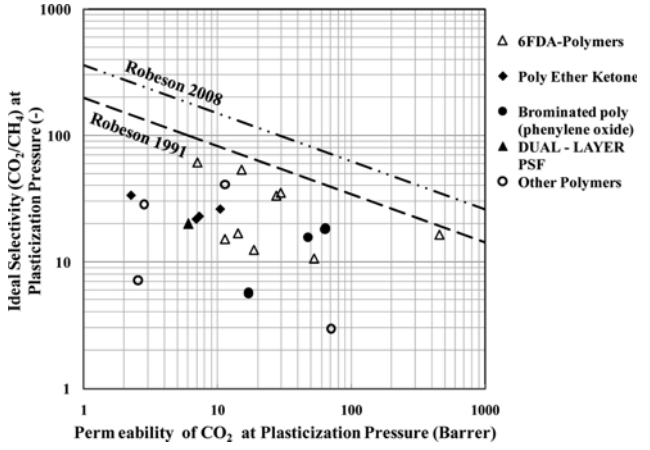

Fig. 3. Ideal selectivity of CO_2/CH_4 and permeability of CO_2 at plasticization pressure. Robeson 2008 (— · · —), Robeson 1991 (— — —).

In addition to other factors, these materials have been chosen due to the availability of experimental data that were in agreement with the developed models and suitable for use in the present study.

PERMEABILITY-PRESSURE RELATIONSHIP OF THE MEMBRANES

Three membranes were selected for the modeling. Permeability equations of those polymers are as follows:

Poly (ether ketone) [47]

CO_2: $P_{CO_2}=0.0008p_{CO_2}^2-0.0997p_{CO_2}+5.3637$ (28)

CH_4: $P_{CH_4}=0.00003p_{CH_4}^2-0.003p_{CH_4}+0.254$ (29)

6FDA-durene polyimide (Dense flat films) [43]:

CO_2: $P_{CO_2}=2.9175p_{CO_2}^2-62.083p_{CO_2}+786.62$ (30)

CH_4: $P_{CH_4}=-0.676p_{CH_4}+34.88$ (31)

6FDA-DAM : DABA 2 : 1 Polyimide [75]:

CO_2: $P_{CO_2}=0.0203p_{CO_2}^2-1.6926p_{CO_2}+85.938$ (32)

CH_4: $P_{CH_4}=1.6885$ (33)

Ideal perm-selectivity:

The ideal selectivity of all the polymers can be expressed as:

$$\alpha_{CO_2/CH_4}=\frac{P_{CO_2}}{P_{CH_4}} \quad (34)$$

PROCESS MODELING AND ANALYSIS OF MEMBRANE PERFORMANCE

1. Process Modeling of Membrane Based Gas Separation

Commercial membrane separation systems are usually packaged as elements or bundles. The most commonly used of these elements for NG processing are the spiral wound and the hollow fibers [19]. In the present study, the spiral wound was assumed due to the types of membranes whose experimental data were used. Fig. 4 is

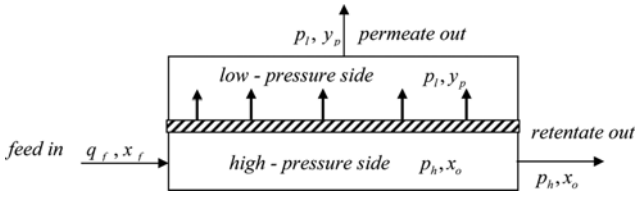

Fig. 4. Process flow diagram of membrane system.

Table 4. Selected membrane materials for illustrative case study

Polymeric membrane	p_{pl} (bar)	$P(p_{pl})$ (Barrer)	$\Delta P(p_{pl})$ (-)	Reference	Reason for selection
PEK (12H)	62.31	2.26	0.579	[47]	Highest plasticization resistance property
6FDA-DAM : DABA 2 : 1	41.69	50.66	0.411	[46]	Lowest productivity loss at plasticization pressure
6FDA-durene polyimide	10.64	456.35	0.420	[43]	Highest permeability at plasticization pressure Highest ideal selectivity at plasticization pressure

p_l is plasticization pressure; $P(p_{pl})$ is permeability at plasticization pressure

PEK (12H): Poly (ether ketone)

6FDA-DAM : DABA 2 : 1: polyimide monoesterified with cyclohexanedimethanol (CHDM) and annealed at 295 °C

Table 5. Economic parameters [21,76]

Parameters	Value	Unit
Membrane cost	50	$/m^2
Membrane replacement cost	54	$/m^2
Membrane life	2-7	year

a schematic representation of complete mixing module used in this study. Table 5 contains the economic parameters used in the present study.

Modeling is done based on the following simplifying assumptions:

i) Steady state conditions

ii) Isothermal conditions (same temperature at every point of the membrane)

iii) Isobaric condition in each membrane compartment (negligible pressure drop on both the upstream and downstream sides)

iv) Concentration-dependent permeability of the penetrant flowing through the membrane

v) Negligible flux coupling (the driving force of each component is its partial pressure difference)

vi) Perfect mixing flow pattern on both the upstream and the downstream sides

Process conditions used include:

Gas flow rate: 35MMSCFD (million std ft^3/day)

Feed composition (x_f): 5-50 mole% CO_2, Balance CH_4

Membrane thickness (l): 50-75 μm

Feed pressure (p_h): 5-140 bar

Permeate pressure (p_l): 1.5 bar

Temperature (T): 35 °C

The following basic equations can be derived from the process flow diagram of Fig. 4.

Permeate mole fraction of CO_2:

$$y_p = \frac{-b + \sqrt{b^2 - 4ac}}{2a} \tag{35}$$

$$a = 1 - \alpha^* \tag{36}$$

$$b = \frac{p_h}{p_l}(1 - x_o) - 1 + \alpha^* \frac{p_h}{p_l} x_o + \alpha^* \tag{37}$$

$$c = -\alpha^* \frac{p_h}{p_l} x_o \tag{38}$$

Membrane Area

$$A_m = \frac{\theta q_f y_p}{\left(\frac{P}{l}\right)(p_h x_o - p_l y_p)} \tag{39}$$

Stage-Cut Equivalent

$$\theta = \frac{q_p}{q_f} \tag{40}$$

Gas Processing Cost

The gas processing cost was calculated using the model given in Eqs. (41)-(42) [17,77]. The equation was modified to include the effect of feed gas pressure.

$$GPC(p_h) = (1.32C_1 + C_2)A_m + 1.4368C_4 q_f + 764245.6806C_5(1 - y_p)q_p \tag{41}$$

The CH_4 loss was calculated using the following equation [21]:

$$CH_4 \text{ loss} = \left(1 - \frac{CH_{4s}}{CH_{4f}}\right) \times 100, \tag{42}$$

where CH_{4s} and CH_{4f} are concentration of CH_4 in the sweet and the feed streams.

2. Performance Analysis of the Membranes

Some of the important design parameters that need to be considered in design of membrane based CO_2 removal from natural gas are membrane area required to achieve desired product purity, and the extent of methane loss. These factors are directly attributed to the overall gas processing cost. One of the process conditions that has direct influence on the design parameters is feed pressure [19]. In this section, the sensitivity of feed pressure is assessed in terms of partial pressure of the plasticizing component of the feed gas.

Fig. 5 shows the effect of the pressure on membrane area. It was explained earlier that increase in pressure causes a decrease in permeability of CO_2. The pressure increase also brings about increase in the driving force. Consequently, the required area is reduced as shown in the figure for all the membranes. There is a sharp drop in the required area at the initial stages of pressure increase. The membrane of 6FDA-Durene has the lowest membrane area requirement. This is because it has the highest permeability among all the

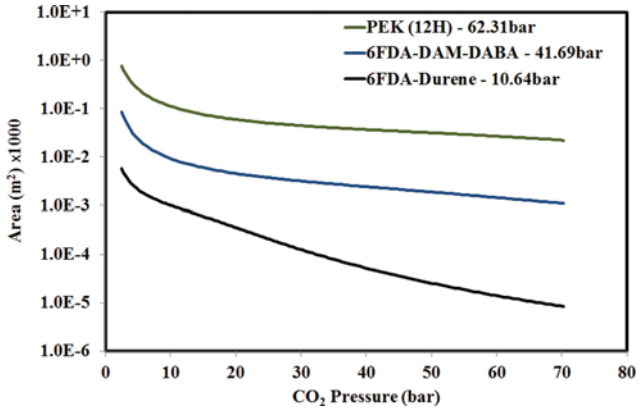

Fig. 5. Effect of pressure on membrane area.

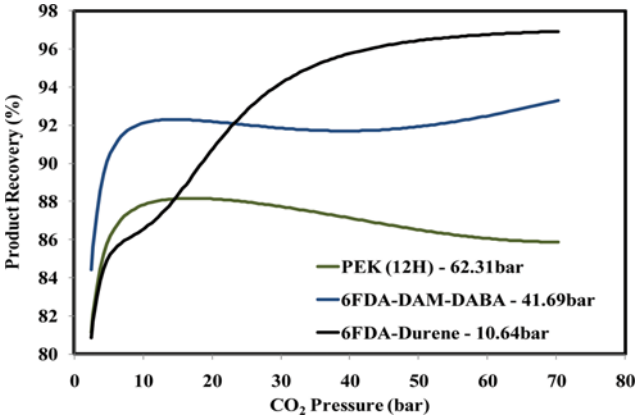

Fig. 6. Effect of pressure on product recovery.

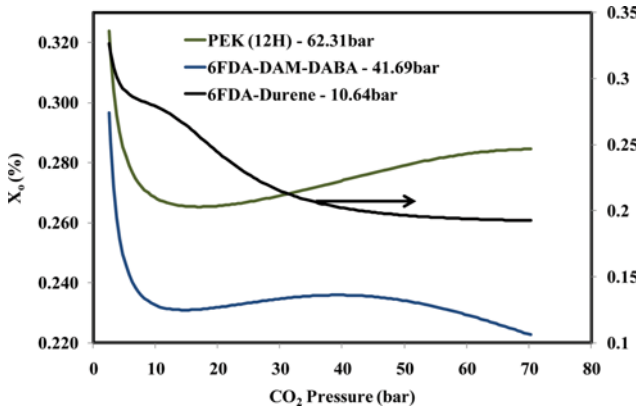

Fig. 7. Effect of pressure on product purity.

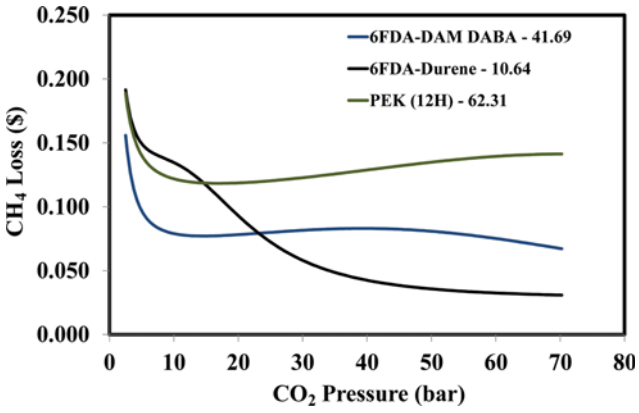

Fig. 8. Effect of pressure on methane loss.

membranes. Conversely, PEK (12) has the highest required area because it is the least permeable of all the membranes. The effect of feed pressure on product recovery is shown in Fig. 6. The most permeable of the membrane (6FDA-Durene) has the highest product recovery of about 97% at 50 bar, which is far higher than its plasticization pressure. The trend continues for other parameters such as product purity, methane loss and overall gas processing costs. 6FDA-Durene was observed to have the best performance result. One other very important observation from all the figures is the decline in the performance observed at CO_2 pressure around the plasticization pressure of the membranes. This observation is more obvious for PEK (12H) and 6FDA-DAM : DABA 2 : 1. For 6FDA - Durene, there seems to be a slight perturbation in the trend of its performance owing to a sharp pressure increase to 6 bars (Fig. 6). The sharp increment is immediately followed by a very slow incremental margin of 5 bar, thereby reaching about 11 bar. Afterwards, the product recovery increases significantly and does not appear to reach steady state until 70 bar. For the other two membranes, there appears to be a decline in their individual performance above the plasticization pressure (Fig. 6 to Fig. 8). Since the available equations commonly used to model gas permeation in membranes do not consider the effect of plasticization, model results beyond the plasticization pressure are considered unreliable. This is evident from the experimental values that are available in the literature on membrane performance beyond the plasticization pressure. The plasticization phenomenon is known to be associated with protracted polymer chain relaxation, which often leads to an increase in permeability, reduction in separation efficiency, unstable and unpredictable membrane performance, and increased loss of revenue (methane loss) due to decline in membrane permselectivity [53].

The limit imposed by the plasticization pressure on high pressure membrane based CO_2 removal from NG was discussed earlier. Evidence of the effect of high-pressure operation above the plasticization pressure was demonstrated from a practical point of view using the combination of experimental results from the literature and those obtained from our laboratory. In general, results from the above figures reveal that there seems to be some improvement in the membrane performance after the plasticization pressure. This is contrary to the experimental finding that was discussed in the previous sections. Indeed, this looks like more of a pseudo improvement because it contradicts experimental findings. At high pressure, polymer matrix swells due high CO_2 concentration within the matrix. This leads to simultaneous increase in CO_2 and CH_4 permeability. The dynamic nature of change in permeability has been studied by many authors as described previously. Below the plasticization pressure, membrane permeability assumes steady state almost immediately after a pressure change. Above the plasticization pressure, experimental results showed that steady state permeability is often protracted. In fact, no steady state was achieved within the experimental time. In some cases, a permeability increment of about 40% was reported within short period of time [42]. Continuous increase in permeability with time causes selectivity loss and the operation becomes economically inefficient. Consequently, membrane materials need to be replaced due to shorter life span (as shown in Table 6). Results from this table

Table 6. Effect of membrane life time on the annual gas processing cost

Membrane life time (year)	Annual gas processing cost ($)		
	PEK (12H)	6FDA-DAM : DABA 2 : 1	6FDA-durene
2.00	1,121,186.13	106,566.24	47,246.60
3.00	888,392.24	85,586.22	38,684.26
4.00	771,995.29	75,096.21	34,403.10
5.00	702,157.12	68,802.20	31,834.40
7.00	655,598.35	64,606.20	28,898.74
10.00	622,342.08	61,609.06	26,697.00

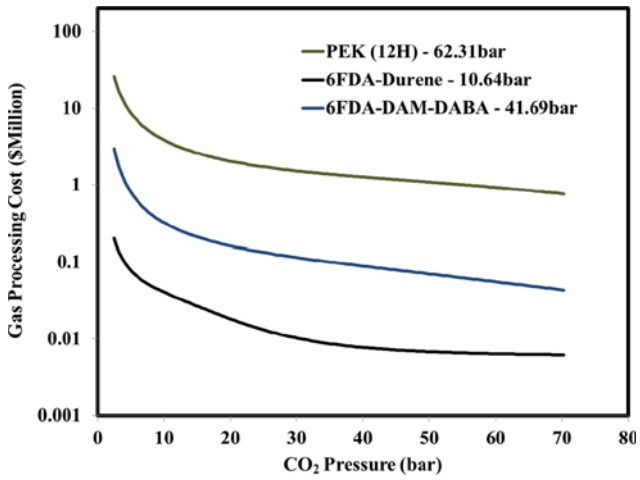

Fig. 9. Effect of pressure on gas processing.

show that annual gas processing increases with membrane lifetime. In addition, the high CO_2 concentration within the polymer film disrupts its chain packing and causes the free volume as well as the segmental mobility to increase [78]. It is believed that the molecular structure of the plasticized membrane is now different from that of the unplasticized one. Thus, we concluded that the present model that is currently in use for the evaluation has some limitations when used at high pressure for separating highly plasticizing gas such as CO_2. On the other hand, the model behavior for the cost of gas processing (GPC) is because GPC is dominated by membrane area (Fig. 9). The model that was used to calculate membrane area failed to capture the effect of membrane plasticization. Also, permeability calculations are based on a steady state assumption, which is only justified at low pressure and pressure below the plasticization pressure of polymers. This limitation can only be rectified by incorporating the effect of plasticization phenomenon into the model. From optimization point of view, this task can be achieved by setting the plasticization pressure as one of the constraints in the optimization model. Thus, in the present work, the high pressure membrane based optimization involving plasticizing feed stream is modeled with a nonlinear constraint optimization model to cater for the identified limitations.

MEMBRANE PROCESS OPTIMIZATION

1. Optimization Model

$$\text{Minimize: } GPC(p_h) \tag{43}$$

$$\text{Subject to: } p_h \le (1-x_f)p_{pl} \tag{44}$$

$$x_{fl} \le x_f \le x_{fh} \tag{45}$$

The optimization was handled using Eqs. (43) and (44) and the economic model of Eqs. (35) to (42). A sensitivity analysis was then performed on the optimum process variables using the second constraint of Eq. (45). The optimization was implemented using the Generalized Reduced Gradient (GRG2) non - linear optimization algorithm [79,80].

2. Single Stage Configuration

Table 7 contains the optimum values of process variables that were obtained from the optimization of a single stage configuration. Based on the results of product purity (x_{o_opt}), 6FDA-DAM : DABA 2 : 1 membrane is the best of the three membranes. However, considering the relative gas processing cost ($RGPC_{opt}$), 6FDA-durene is the most economical membrane. This outcome is in line with the outcome of previous similar optimization studies that concluded that there is no unique optimum [17]. The lowest value of the optimum product purity of 6FDA-DAM : DABA 2 : 1 is due to its selectivity, which is the highest among the three membranes. 6FDA-durene has the lowest optimum gas processing cost due to its lowest area requirement resulting from its highest permeability at plasticization pressure. One of the interesting results from this table is the value of x_{o_opt} for PEK (12H) and 6FDA-durene. Both polymers have very contrasting properties: PEK (12H) has the highest plasticization pressure but the lowest permeability at plasticization; however, 6FDA-durene has the lowest plasticization pressure but highest permeability at plasticization. Yet, both polymers have almost the same value of optimum product purity. This is actually an indication that both of these properties are equally important in the optimization of high pressure membrane based CO_2 removal from natural gas. This fact is corroborated by the optimum process variable value for 6FDA-DAM : DABA 2 : 1 membrane whose plasticization pressure and permeability at plasticization are between those of the two polymers. Thus, future research work needs to be focused on improving these two properties.

Typical pipeline specification of natural gas is in the range of 2-5 mol% [17,19,81]. The results in Table 7 also indicate that none of the membranes could process crude NG containing 50 mol% CO_2 to this range of specification using the single stage configuration. This is due to the high concentration of the acid gas in the feed. Thus, a second stage is needed to treat such feed gas in order to obtain pipeline specifications. For this purpose, a sensitivity analysis of the feed composition on the product purity and gas processing cost was first performed to find the range of feed gas composition that could be processed with single stage in order to obtain the pipeline specifications. Secondly, further modeling was performed to determine if a second stage configuration can be used

Table 7. Optimum values of process variables for processing 35MMCFD of 50 mol% CO_2 natural gas

Membrane	p_{pl} (bar)	p_{h_opt} (bar)	CO_2 P_{opt} (Barrer)	α_{opt} (-)	x_{o_opt} (-)	$RGPC_{opt}$ (-)	$A_m \times 1000$ (m^2)
PEK (12H)	62.31	124.62	2.257	12.30	0.283	36.02	25.95
6FDA-DAM : DABA 2-1	41.69	83.38	50.656	30.00	0.236	15.02	2.34
6FDA-durene	10.64	21.28	456.346	16.48	0.277	1.00	0.95

Table 8. Sensitivity of feed composition to the purity of the product

Feed composition (mol% CO_2)	CO_2 concentration in the retentate (mol%)		
	PEK (12H)	6FDA-DAM : DABA 2 : 1	6FDA-durene
5	0.90	0.50	1.10
10	2.10	1.10	2.30
15	3.60	1.90	3.80
20	5.50	3.00	5.60
25	7.90	4.40	7.70
30	10.80	6.40	10.40
35	14.30	9.20	13.70
40	18.50	13.00	17.70
45	23.10	17.80	22.40
50	28.30	23.60	27.70

to achieve the desired specification. Results of the sensitivity analysis are shown on Table 8. From the table, it is revealed that both the PEK (12H) and 6FDA-durene are suitable for processing natural gas with about 18.5 mol% CO_2 feed composition to obtain the pipeline specification range. Raw natural gas containing about 27 mol% CO_2 in the feed gas is better processed using 6FDA-DAM : DABA 2 : 1 membrane. For raw natural gas with higher CO_2 than this, product purity of 5 mol% CO_2 can be attained by either using membrane with higher plasticization pressure and permeability parameters at plasticization or use of multistage configurations. Feed and product compositions of the three membranes are shown in Table 9.

From this table, the raw natural gas was purified to about half its initial concentration. These results revealed the capability of the single stage configuration to be used for bulk natural gas processing in the off shore platform of crude oil exploration where space is a very important economic factor.

The gas processing cost of natural gas using amine absorption and single stage membrane separation was reported as 0.18 and 0.08 $Million/MSCF product, respectively [21]. Thus, in order to reduce cost, the single stage can be used in area of process plant retrofitting with other equipment (such as absorber) to form a hybrid separation process.

3. Two Stage Configurations

This work was meant to be focused on how to optimize single stage configuration to process natural gas to the pipeline specification standard; however, how the optimized single stage configuration is combined to achieve desired gas purity needs to be discussed. Based on the properties of the available membrane, additional stages will be needed to attain the commonly required pipeline specifications. Based on the results of Table 9, a two-stage configuration was modeled using 6FDA-DAM : DABA 2 : 1 membrane to process the retentate that comes from the first stage. Results of this modeling are shown in Table 10. Results from the table show that 6FDA-DAM : DABA 2 : 1 membrane in a two stage configuration can be used to process a natural gas feed with 50 mol% CO_2 to a pipeline specification between 2-5 mol%.

Table 10. Optimum feed and product composition for the second stage

Membrane material	Feed (mol%)		Product (mol%)	
	CH_4	CO_2	CH_4	CO_2
6FDA-DAM : DABA 2 : 1	76.42	23.58	96.05	3.95

CONCLUSIONS

Systematic process design, modeling and optimization of high pressure membrane based removal of CO_2 from natural gas were performed on selected polymeric membranes (PEK (12H), 6FDA-DAM : DABA 2 : 1 and 6FDA-durene). Selection criteria, which included plasticization pressure and permeability parameters (permeability, selectivity and productivity loss) at plasticization, were used in conjunction with the upper bound curve that was modified for high pressure operations.

It was observed that high pressure membrane based CO_2 removal is more economical than the low pressure. The plasticization pressure and the permeability at plasticization are very important factors in the operation. Using the plasticization pressure as constraints, gas processing costs were $ 4,613,094.47, 421,266.49 and 175,681.60 for PEK (12H), 6FDA-DAM : DABA 2 : 1 and 6FDA-durene membranes, respectively. Membrane with the highest permeability has the lowest membrane area, and hence the lowest optimum gas processing cost. The 6FDA-DAM : DABA 2 : 1 membrane, whose plasticization pressure and permeability values lie between the other two membranes, has the highest product purity. Using this membrane to process a natural gas with 50 mol% CO_2 concentration, a two-stage membrane configuration is needed to achieve the pipeline specification range of 2-5 mol%.

Studies on the steady state and dynamic process modeling of multistage configurations, identification of optimum process conditions, and the effects of recycle on both the single and multistage high pressure CO_2 removal from natural gas are recommended future studies.

Table 9. Feed and product compositions at the optimum process conditions

Membrane material	Feed composition (mol%)		Product composition (mol%)				Product recovery
			Permeate		Retentate		
	CH_4	CO_2	CH_4	CO_2	CH_4	CO_2	
6FDA-DAM : DABA 2 : 1	50	50	10.369	89.631	76.421	23.579	91.71
6FDA-durene	50	50	16.528	83.472	72.315	27.685	86.78
PEK (12H)	50	50	17.517	82.483	71.655	28.345	85.99

ACKNOWLEDGEMENT

The authors gratefully acknowledge the support of the Membrane Cluster Research Group, Universiti Sains Malaysia, and Center for Petroleum & Minerals, King Fahd University of Petroleum & Minerals, Saudi Arabia.

NOMENCLATURE

6FDA : (4,40-Hexafluoroisopropylidene) diphthalic anhydride
A_m : membrane area [m^2]
a_1, a_2, a_3 : model constants
b : hole affinity constant
C : concentration of the diffusing species across the membrane
C_1 : membrane module manufacturing cost [$/$m^2$]
C_2 : membrane replacement costs [$/$m^2$]
C_3 : energy cost (EC) [$/kW-hr]
C_4 : labor cost [$/hr]
C_5 : cost of hydrocarbon loss [$/MMBTU]
C_D : gas concentration due ordinary dissolution (which obeys Henry's law)
C_H : gas concentration due to micro cavities or holes (which obeys the Langmuir Isotherm)
C_h : concentration of CO_2 on the upstream
C'_H : saturation concentration of the penetrant species in the polymer micro cavities
CH_{4f} : concentration of CH_4 in the feed streams
CH_{4s} : concentration of CH_4 in the sweet streams
C_l : concentration of CO_2 on the low pressure side
D : diffusion coefficient
DAM : 2,4,6-trimethyl-1,3-diaminobenzene
DABA : 3,5-diaminobenzoic acid
D_0 : diffusion coefficient at zero concentration in the polymer matrix
F : fraction of Langmuir sorption species having a finite mobility
GPC : gas processing cost
J : gas flux
k : constant parameter
k_D : solubility coefficient in the Henry's law limit
l : membrane thickness [m]
P : permeability of fast gas (CO_2)
p : gas pressure [bar]
PEK : poly (ether ketone)
p_h : feed/upstream gas pressure [bar]
p_l : downstream/permeate gas pressure [bar]
p_{pl} : plasticization pressure [bar]
Q : quantity of diffusing gas
q_f : feed flow rate in kmol/s
q_p : permeate flow rate in kmol/s
q_r : retentate flow rate in kmol/s
t : time
t_m : membrane life [years]
x_o : concentration of CO_2 in the retentate (product) [mol%]
(x_f) : feed composition
y_p : concentration of CO_2 in the permeate [mol%]

Greek Letters

α_{AB} : selectivity of the fast gas with respect to the slow gas
$: US Dollar
θ : stage - cut
φ : empirical parameter representing the extent of the concentration dependence of the diffusion

Subscript

mob : mobile
mobh : mobile at high pressure side

Superscript

n : constant parameter

REFERENCES

1. T. M. Murphy, G. T. Offord and D. R. Paul, In Membrane Operations. Innovative Separations and Transformations; Drioli, E., Giorno, L., Eds., WILEY-VCH Verlag GmbH & Co. KGaA: Weinheim (2009).
2. W. B. Baker, *J. Membr.*, **362**, 134 (2010).
3. L. Giorno, G. De Luca, A. Figoli, E. Piacentini and E. Drioli, In Membrane Operations, Wiley-VCH Verlag GmbH & Co. KGaA (2009).
4. A. Criscuoli, In Membrane Operations, Wiley-VCH Verlag GmbH & Co. KGaA (2009).
5. R. T. Adams, J. S. Lee, T. H. Bae, J. K. Ward, J. R. Johnson, C. W. Jones, S. Nair and W. J. Koros, *J. Membr. Sci.*, **367**, 197 (2011).
6. A. L. Ahmad, J. K. Adewole, C. P. Leo, S. Ismail, A. S. Sultan and S. O. Olatunji, *J. Membr. Sci.*, **480**, 39 (2015).
7. Y. Xiao, B. T. Low, S. S. Hosseini, T. S. Chung and D. R. Paul, *Progress in Polymer Science*, **34**, 561 (2009).
8. J. K. Adewole, A. L. Ahmad, S. Ismail and C. P. Leo, *Int. J. Greenh. Gas. Con.*, **17**, 46 (2013).
9. C. A. Scholes, G. Q. Chen, G. W. Stevens and S. E. Kentish, *J. Membr. Sci.*, **346**, 208 (2010).
10. T.-S. Chung, C. Cao and R. Wang, *J. Polym. Sci., Part B: Polym. Phys.*, **42**, 354 (2004).
11. R. Spillman, In Membrane Science and Technology, Richard, D. N., Stern, S. A., Eds., Elsevier (1995).
12. B. D. Bhide and S. A. Stern, *J. Membr. Sci.*, **81**, 209 (1993).
13. R. Qi and M. A. Henson, *J. Membr. Sci.*, **121**, 11 (1996).
14. R. Qi and M. A. Henson, *Sep. Purif. Technol.*, **13**, 209 (1998).
15. J. Hao, P. A. Rice and S. A. Stern, *J. Membr. Sci.*, **320**, 108 (2008).
16. J. Hao, P. A. Rice and S. A. Stern, *J. Membr. Sci.*, **209**, 177 (2002).
17. A. K. Datta and P. K. Sen, *J. Membr. Sci.*, **283**, 291 (2006).
18. D. Yang, Z. Wang, J. Wang and S. Wang, *Ind. Eng. Chem. Res.*, **48**, 9013 (2009).
19. M. Safari, A. Ghanizadeh and M. M. Montazer-Rahmati, *Int. J. Greenh. Gas. Con.*, **3**, 3 (2009).
20. F. Ahmad, K. K. Lau, A. M. Shariff and G. Murshid, *Comput. Chem. Eng.*, **36**, 119 (2012).
21. L. Peters, A. Hussain, M. Follmann, T. Melin and M. B. Hagg, *Chem. Eng. J.*, **172**, 952 (2011).
22. A. Bos, I. G. M. Pünt, M. Wessling and H. Strathmann, *J. Membr. Sci.*, **155**, 67 (1999).

23. B. D. Bhide and S. A. Stern, *J. Membr. Sci.*, **62**, 13 (1991).
24. J. Vaughn and W. J. Koros, *Macromolecules*, **45**, 7036 (2012).
25. A. Bos, I. G. M. Pünt, M. Wessling and H. Strathmann, *J. Polym. Sci., Part B: Polym. Phys.*, **36**, 1547 (1998).
26. J. G. Wijmans and R. W. Baker, *J. Membr. Sci.*, **107**, 1 (1995).
27. B. Flaconnèche, J. Martin and M. H. Klopffer, *Oil Gas Sci. Technol. - Rev. IFP*, **56**, 245 (2001).
28. A. L. Ahmad, J. K. Adewole, S. B. Ismail, L. C. Peng and A. S. Sultan, *Defect Diffus Forum*, **333**, 135 (2013).
29. W. R. Vieth, Diffusion In Model and Through Polymers, Hanser Publishers, New York (1991).
30. W. J. Koros, D. R. Paul and A. A. Rocha, *J. Polym. Sci., Part B: Polym. Phys.*, **14**, 687 (1976).
31. D. R. Paul and W. J. Koros, *J. Polym. Sci., Part B: Polym. Phys.*, **14**, 675 (1976).
32. M. H. Klopffer and B. Flaconnèche, *Oil Gas Sci. Technol. - Rev. IFP*, **56**, 223 (2001).
33. J. S. McHattie, W. J. Koros and D. R. Paul, *Polymer*, **32**, 2618 (1991).
34. J. S. McHattie, W. J. Koros and D. R. Paul, *Polymer*, **32**, 840 (1991).
35. J. S. McHattie, W. J. Koros and D. R. Paul, *Polymer*, **33**, 1701 (1992).
36. A. Y. Houde, S. S. Kulkarni and M. G. Kulkarni, *J. Membr. Sci.*, **95**, 147 (1994).
37. K. M. P. Kamps, H. A. Teunis, M. Wessling and C. A. Smolders, *J. Membr. Sci.*, **74**, 193 (1992).
38. H. Kumazawa, J. S. Wang, T. Fukuda and E. Sada, *J. Membr. Sci.*, **93**, 53 (1994).
39. R. Srinivasan, S. R. Auvil and P. M. Burban, *J. Membr. Sci.*, **86**, 67 (1994).
40. R. Wang, S. L. Liu, T. T. Lin and T. S. Chung, *Chem. Eng. Sci.*, **57**, 967 (2002).
41. S. A. Stern and V. Saxena, *J. Membr. Sci.*, **7**, 47 (1980).
42. A. Bos, I. G. M. Pünt, M. Wessling and H. Strathmann, *Sep. Purif. Technol.*, **14**, 27 (1998).
43. W.-H. Lin and T.-S. Chunga, *J. Membr. Sci.*, **186**, 183 (2001).
44. X. Chen, D. Rodrigue and S. Kaliaguine, *Sep. Purif. Technol.*, **86**, 221 (2012).
45. B. Kraftschik, W. J. Koros, J. R. Johnson and O. Karvan, *J. Membr. Sci.*, **428**, 608 (2013).
46. J. D. Wind, S. M. Sirard, D. R. Paul, P. F. Green, K. P. Johnston and W. J. Koros, *Macromolecules*, **36**, 6433 (2003).
47. J. M. Mohr, D. R. Paul, G. L. Tullos and P. E. Cassidy, *Polymer*, **32**, 13, 2387 (1991).
48. A. Bos, I. G. M. Pünt, M. Wessling and H. Strathmann, *J. Membr. Sci.*, **155**, 67 (1999).
49. A. Bos, I. G. M. Pünt, M. Wessling and H. Strathmann, *Sep. Purif. Technol.*, **14**, 27 (1998).
50. A. Y. Houde, B. Krishnakumar, S. G. Charati and S. A. Stern, *J. Appl. Polym. Sci.*, **62**, 2181 (1996).
51. M. R. Pixton and D. R. Paul, *Polymer*, **36**, 3165 (1995).
52. A. M. Kratochvil and W. J. Koros, *Macromolecules*, **41**, 7920 (2008).
53. J. D. Wind, S. M. Sirard, D. R. Paul, P. F. Green, K. P. Johnston and W. J. Koros, *Macromolecules*, **36**, 6442 (2003).
54. H. Kumazawa, K. Inamori, B. Messaoudi and E. Sada, *J. Membr. Sci.*, **97**, 7 (1994).
55. R. T. Chern, F. R. Sheu, L. Jia, V. T. Stannett and H. B. Hopfenberg, *J. Membr. Sci.*, **35**, 103 (1987).
56. T. Nakagawa, T. Nishimura and A. Higuchi, *J. Membr. Sci.*, **206**, 149 (2002).
57. L. Zhang, Y. Xiao, T. S. Chung and J. Jiang, *Polymer*, **51**, 4439 (2010).
58. F. A. Ruiz-Treviño and D. R. Paul, *J. Appl. Polym. Sci.*, **68**, 403 (1998).
59. W. Qiu, C.-C. Chen, L. Xu, L. Cui, D. R. Paul and W. J. Koros, *Macromolecules*, **44**, 6046 (2011).
60. A. L. Khan, X. Li and I. F. J. Vankelecom, *J. Membr. Sci.*, **372**, 87 (2011).
61. P. S. Tin, T. S. Chung, Y. Liu, R. Wang, S. L. Liu and K. P. Pramoda, *J. Membr. Sci.*, **225**, 77 (2003).
62. A. M. W. Hillock and W. J. Koros, *Macromolecules*, **40**, 583 (2007).
63. C. E. Powell, X. J. Duthie, S. E. Kentish, G. G. Qiao and G. W. Stevens, *J. Membr. Sci.*, **291**, 199 (2007).
64. B. T. Low, T. S. Chung, H. Chen, Y.-C. Jean and K. P. Pramoda, *Macromolecules*, **42**, 7042 (2009).
65. M. J. Reimers and T. A. Barbari, *J. Polym. Sci. Part B: Polym. Phys.*, **32**, 131 (1994).
66. C.-C. Hu, Y.-J. Fu, K.-R. Lee, R.-C. Ruaan and J.-Y. Lai, *Polymer*, **50**, 5308 (2009).
67. L. M. Robeson, *J. Membr. Sci.*, **62**, 165 (1991).
68. B. D. Freeman, *Macromolecules*, **32**, 375 (1999).
69. L. M. Robeson, H. H. Hwu and J. E. McGrath, *J. Membr. Sci.*, **302**, 70 (2007).
70. L. M. Robeson, *J. Membr. Sci.*, **320**, 390 (2008).
71. A. Y. Alentiev and Y. P. Yampolskii, *J. Membr. Sci.*, **165**, 201 (2000).
72. B. W. Rowe, L. M. Robeson, B. D. Freeman and D. R. Paul, *J. Membr. Sci.*, **360**, 58 (2010).
73. L. M. Robeson, Z. P. Smith, B. D. Freeman and D. R. Paul, *J. Membr. Sci.*, **453**, 71 (2014).
74. S. Kanehashi, T. Nakagawa, K. Nagai, X. Duthie, S. Kentish and G. Stevens, *J. Membr. Sci.*, **298**, 147 (2007).
75. J. D. Wind, S. M. Sirard, D. R. Paul, P. F. Green, K. P. Johnston and W. J. Koros, *Macromolecules*, **36**, 6433 (2003).
76. R. W. Baker, In Membrane Technology and Applications, John Wiley & Sons, Ltd. (2004).
77. L. Peters, A. Hussain, M. Follmann, T. Melin and M. B. Hägg, *Chem. Eng. J.*, **172**, 952 (2011).
78. A. Bos, I. G. M. Pünt, M. Wessling and H. Strathmann, *J. Polym. Sci., Part B: Polym. Phys.*, **36**, 1547 (1998).
79. T. F. Edgar, D. M. Himmelblau and L. S. Lasdon, Optimization of Chemical Processes, McGraw-Hill, New York (2001).
80. S. S. Rao and S. S. Rao, Engineering Optimization: Theory and Practice, John Wiley & Sons, New Jersey (2009).
81. J. K. Adewole, A. L. Ahmad, A. S. Sultan, S. Ismail and C. P. Leo, *J. Polym. Res.*, **22**, 1 (2015).